

Chemical and Thermal Equilibration of QGP in Heavy Ion Collisions.

HU – IITB Workshop 21 February 2023

Cendikia Abdi
Sohaken, Hiroshima University.
Supervisor: Chiho Nonaka.

Introduction

Phase Diagram

of Quantum Chromodynamics

Early Universe

Quark-Gluon Plasma

Critical point ?

Hadron

Color Superconductivity?

Neutron Star

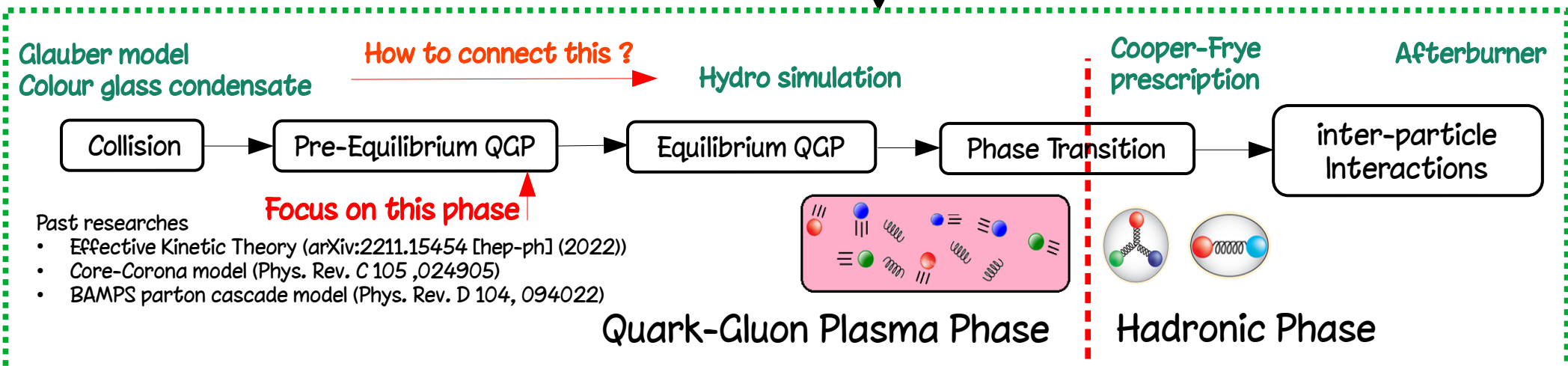
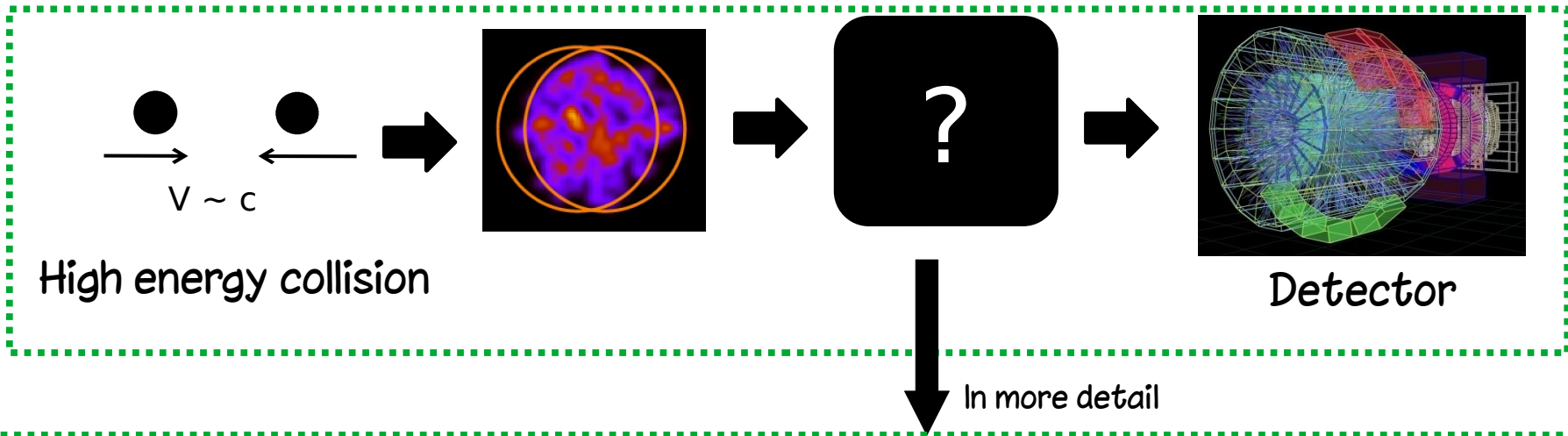
density

Temperature

Area of Focus

- Quark-Gluon Plasma (QGP) is a state of matter where quarks and gluons are decoupled, thus they can move freely.
- Main source of observable QGP comes from high energy particle colliders.

Aim and Goal



Challenge with pre-equilibrium QGP

Why simulating this part is difficult :

- Non equilibrated energetic medium => hydrodynamic and equilibrium statistical mechanic are not applicable.

Solution

Use Kinetic Theory approach (i.e solving Boltzmann Transport Eq)

$$\frac{\partial}{\partial t} f(t, \vec{r}, \vec{p}) + \frac{\vec{p}}{m} \nabla_{\vec{r}} f(t, \vec{r}, \vec{p}) - \nabla_{\vec{r}} U(\vec{r}) \nabla_{\vec{p}} f(t, \vec{r}, \vec{p}) = \left(\frac{\partial f}{\partial t} \right)_{coll}$$

Time evolution

Diffusion

External field

Interparticle collision

Inter particle collision can be written as (example for 2 → 2 collision only) :

$$\text{Rate}(a + b \rightarrow c + d) = \frac{1}{1 + \delta_{ab}} \int \frac{d^3 p_a}{2E_a (2\pi)^3} \frac{d^3 p_b}{2E_b (2\pi)^3} \frac{d^3 p_c}{2E_c (2\pi)^3} \frac{d^3 p_d}{2E_d (2\pi)^3} (2\pi)^4 \delta^4(p_a + p_b - p_c - p_d) |M(a + b \rightarrow c + d)|^2 f_a f_b (1 \pm f_c) (1 \pm f_d).$$

Collision term is the summation of above term for each channel and each particle species

Model description

Let's start simple with Boltzmann Transport Equation only with 2 → 2 process for an example

$$\left(\frac{\partial}{\partial t} + \frac{\vec{p}}{E_a} \nabla_{\vec{r}} - \nabla_{\vec{r}} U(\vec{r}) \nabla_{\vec{p}} \right) f_a(t, \vec{r}, \vec{p}) = \sum_{bcd} \int \frac{d^3 p_b}{2E_b(2\pi)^3} \frac{d^3 p_c}{2E_c(2\pi)^3} \frac{d^3 p_d}{2E_d(2\pi)^3} \\ \times \frac{1}{2E_a} (2\pi)^4 \delta^4(p_a + p_b - p_c - p_d) \left[\frac{1}{1 + \delta_{cd}} |M(c + d \rightarrow a + b)|^2 f_c f_d (1 \pm f_a)(1 \pm f_b) \right. \\ \left. - \frac{1}{1 + \delta_{ab}} |M(a + b \rightarrow c + d)|^2 f_a f_b (1 \pm f_c)(1 \pm f_d) \right],$$

Even in simple case, we have non-linear differential equation which is difficult to solve

Based on Hadronic Transport
Model SMASH^[1]

Approach

Quantum molecular Dynamic
⇒ Monte-Carlo solver
⇒ Approximation solution to
Boltzmann Transport Equation

Simplify the equation

- Effective Kinetic Theory
- Relaxation Time Approximation
- Linearized Boltzmann Equation
- ...

Recent researches related to this subject

- Effective Kinetic Theory*.
Uses QCD-like cross-section, includes elastic $2 \leftrightarrow 2$ and gluon splitting/merging $2 \leftrightarrow 1$ processes up to leading order. Box with periodic boundary condition and fixed $\alpha_s = 0.3$.
Still in preliminary test for equilibrium case.
- Hydrodynamization by hydrodynamic attractor**.
Hydrodynamization refers to the transition between dynamic micro system to hydrodynamic system. This paper approaches hydrodynamization by hydrodynamic attractor

$$\chi = \frac{P_L}{P_T} \quad \text{Which describes momentum anisotropy.}$$

Comparing BAMPS parton cascade, relaxation time approximation, and VSHASTA hydrodynamic simulation, BAMPS and RTA showed similar result while hydrodynamic simulation showed a small deviation. Less interaction always lead to a slower hydrodynamization.

- Most of recent studies using parton cascade focus on jet quenching phenomenon.
Application to hydrodynamization and equilibration process is still rare.

*Aleksi Kurkela, Robin Törnkvist, Korinna Zapp. arXiv:2211.15454 [hep-ph] (2022)

**Victor E. Ambrus, Sergiu Busuioc, Jan A. Fotakis, Kai Gallmeister, Carsten Greiner arXiv:2102.11785v3 [nucl-th] (2021)

SMASH's Workflow

Setting initial position and momentum for each point-particles

Check for collision with stochastic method

$$P_{2 \rightarrow N} = v_{rel} \frac{\sigma_{2 \rightarrow N}}{N_{test}} \frac{\Delta t}{\Delta^3 x} \quad P_{3 \rightarrow 2} = \frac{1}{4E_1 E_2 E_3} \frac{(s - m_1^2 - m_2^2)^2 - 4m_1^2 m_2^2}{\Psi_3 8\pi s} \sigma_{2 \rightarrow 3} \frac{\Delta t}{\Delta^3 x}$$

SMASH limits 1 collision per timestep

Final state sampling

- Replace incoming particles' position and momentum with the sampled final state

Update particles

- Propagate particles in straight lines (Δt assumed to be small enough to ignore force)
- Update potential among particles

- Update momentum based on $\frac{dp}{dt} = E^{\vec{v}} + \vec{v} \times B^{\vec{v}}$

For the sake of simplicity,
consider no external field

Initial Condition

- Initial condition (Glauber Model).

Initial particles are from mini-jets produced by binary collision between nucleons

- Particle number

$$N = 4\nu \sigma_{jet} \int d^2 x_T dz dt n_A(\vec{x}_T, z - vt) n_B(\vec{x}_T, z + vt) \quad \text{with} \quad \sigma_{jet} = \int_{P_{t,cutoff}^2}^{4 P_{CoM}^2} dt \frac{d\sigma}{dt} \quad \text{Miniset cutoff @ 2 GeV and only until leading order}$$

Each collision produces 2 parton x 2 to include higher order perturbation

$$\text{and } n_A(\mathbf{x}_{T1}, z_1) = \frac{\gamma n_0}{1 + \text{Exp}\left(\left(\sqrt{x_{T1}^2} + (\gamma z_1)^2 - R_A\right)/d\right)}$$

With $d = 0.54 \text{ fm}$

$$R_A = 1.12A^{1/3} - 0.86 A^{-1/3}$$

n_0 = normalization constant so that

$$A = \int_0^\infty dr n(r)$$

- Momentum distribution

$$\frac{d\sigma_{jet}}{dp_T^2 dy_1 dy_2} = K \sum_{a,b} x_1 f_a(x_1, p_T^2) x_2 f_b(x_2, p_T^2) \frac{d\sigma_{ab}}{d\hat{t}}$$

With f_1 and f_2 partonic distribution function (NNPDF^[2])

Initial Condition : Numerical Calculation

- Cross section from perturbative QCD up to leading order + small angle approximation.

Elastic collision

$gg \rightarrow gg$

$$\frac{d\sigma_{gg \rightarrow gg}}{dt} = \frac{9\pi\alpha_s^2}{t^2}$$

$qq \rightarrow qq$

$$\frac{d\sigma_{qq \rightarrow qq}}{dt} = \frac{16\pi\alpha_s^2}{9t^2}$$

$gq \rightarrow gq$

$$\frac{d\sigma_{gq \rightarrow gq}}{dt} = \frac{2\pi\alpha_s^2}{t^2}$$

Inelastic collision

$gg \rightarrow qq_{\text{bar}}$

$$\frac{d\sigma_{gg \rightarrow q\bar{q}}}{dt} = \frac{\pi\alpha_s^2}{3st}$$

$qq_{\text{bar}} \rightarrow gg$

$$\frac{d\sigma_{q\bar{q} \rightarrow gg}}{dt} = \frac{64\pi\alpha_s^2}{27st}$$

- Cut-off is employed to avoid infrared divergence $\Rightarrow p_{\text{cut-off}} = 1.8 \text{ GeV}$ (from Au + Au @ 200 GeV PYTHIA)
- Sanity check. From deep inelastic collision

$$\sigma_{pp} = \int dx_1 dx_2 dt \sum_{\text{all channels}} x_1 f_1(x_1) x_2 f_2(x_2) \frac{d\sigma}{dt} = 46.3622 \text{ mb}$$

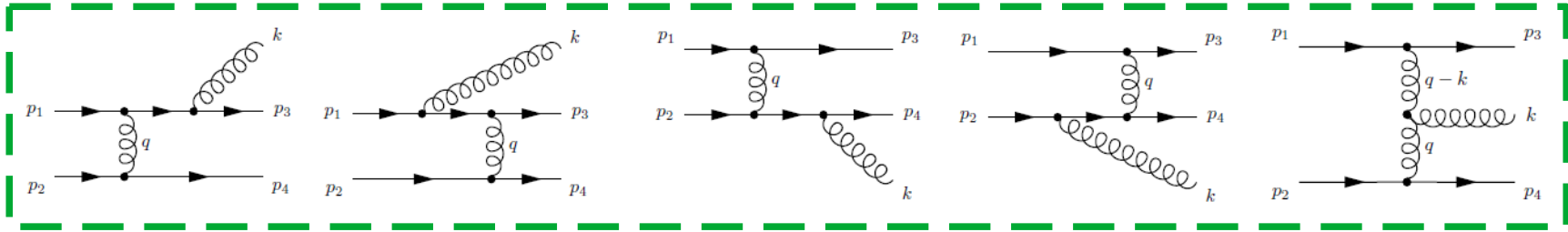
(COMPETE^[3] prediction = 51.79 mb and STAR^[4] experiment = 54.67 mb)

[3] J.R. Cudell, et al., COMPETE Collaboration, Phys. Rev. Lett. 89 (2002) 201801.

[4] STAR Collaboration Physics Letters B 808 (2020) 135663

Improved Gunion-Bertsch cross-section

- The 2-to-3 cross section is calculated using **improved GB approximation**^[5] to speed up calculation. This approximation includes **5 channels** for gluon emission/absorption process.



Points :

- Calculate in CoM frame, in light-cone coordinates, with assumptions

$$k_{\perp} \ll \sqrt{s}, \quad q_{\perp} \ll \sqrt{s}, \quad xq_{\perp} \ll k_{\perp} \text{ with } x = \frac{k_{\perp}}{\sqrt{s}} e^y \Rightarrow \text{soft gluon exchange and soft gluon radiation}$$

- Resulting amplitude can be written as

$$|M_{2 \rightarrow 3}|^2 = 12 g^2 |M_{2 \rightarrow 2}|^2 (1-x)^2 \left[\frac{k_{\perp}}{k_{\perp}^2 + x^2 M^2} + \frac{q_{\perp} - k_{\perp}}{(q_{\perp} - k_{\perp})^2 + x^2 M^2} \right]$$

i.e 2 → 3 amplitude = 2 → 2 amplitude × gluon splitting function

Infrared Divergence Regularization

- Infrared divergence arises from the cross-section calculation due to the interaction amplitude inversely proportional to t squared

$$\sigma \propto \int_0^s dt |M_{2 \rightarrow 2}|^2 \quad \text{with} \quad |M_{2 \rightarrow 2}|^2 \propto \frac{1}{t^2} \simeq \frac{1}{q_\perp^4}$$

- This infrared divergence is avoided by using colour-screening mass in the one-loop approximation* in SU(3) and up to α_s order, with gluon screening mass given by

$$m_D^2 = 16 \pi \alpha_s \frac{\int d^3 p}{(2\pi)^3} \frac{1}{|p|} (N f_g + n_f f_q)$$

and quark screening mass for quark-antiquark to gluon process

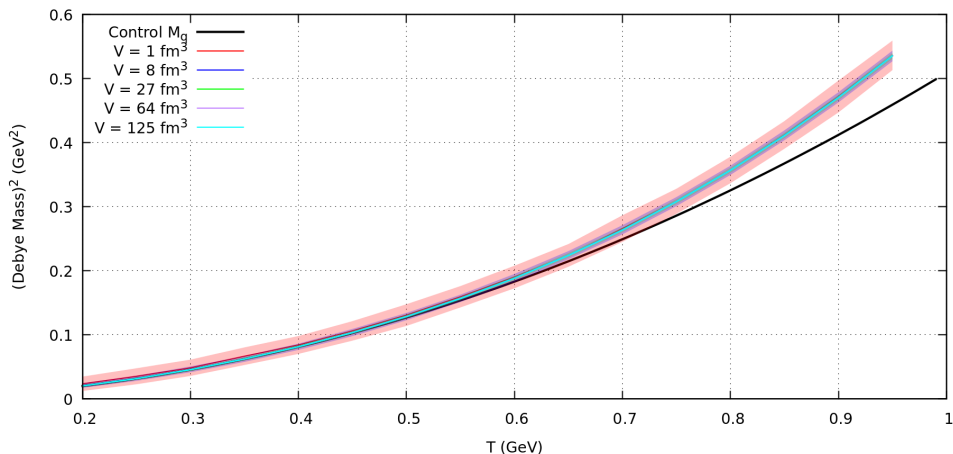
$$m_q^2 = 4 \pi \alpha_s \frac{N^2 - 1}{2N} \frac{\int d^3 p}{(2\pi)^3} \frac{1}{|p|} (f_g + f_q)$$

Which is derived from equilibrium expression applied to non-equilibrium distribution

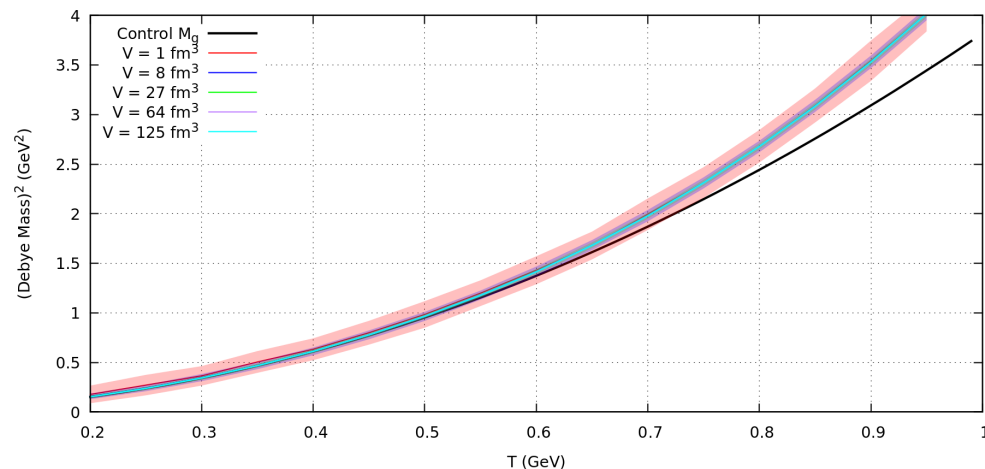
*S. M. H. Wong, Phys. Rev. C 54, 2588 (1996)

Infrared Divergence Regularization

Quark Screening Mass



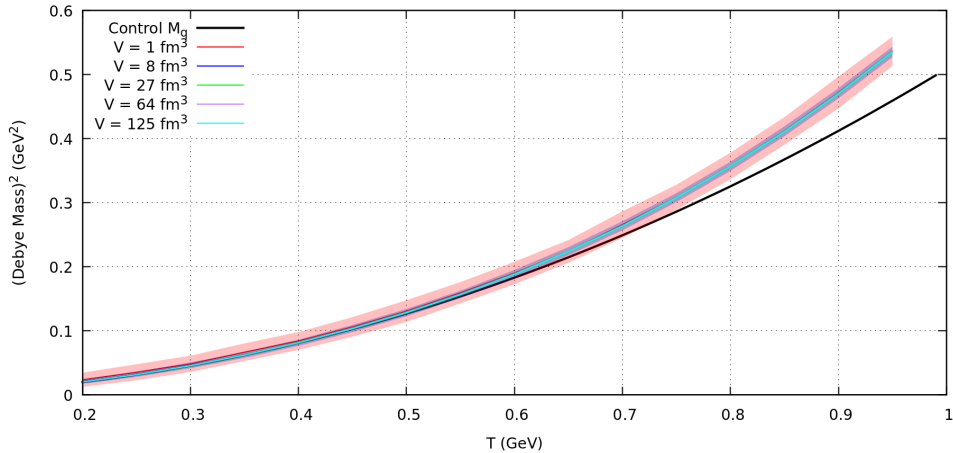
Gluon Screening Mass



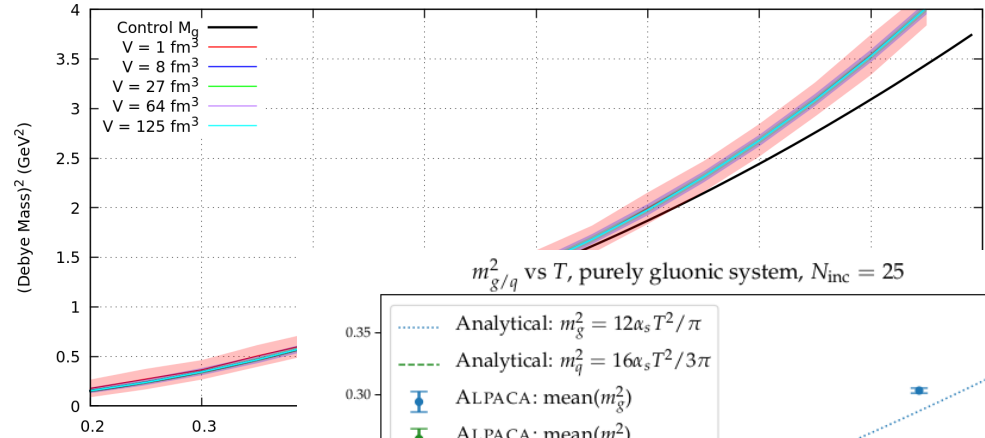
- Applying the screening mass formulation from the previous definition into the medium initiated in an equilibrium state of different temperature and volume showed deviation at higher temperature region.
- Control value is calculated using direct integration assuming equilibrium follows B-E or F-D distribution. In the simulation, we calculated screening mass by discretizing the original formula, thus the deviation is believed to come from the discretization error.

Infrared Divergence Regularization: High T Region Deviation

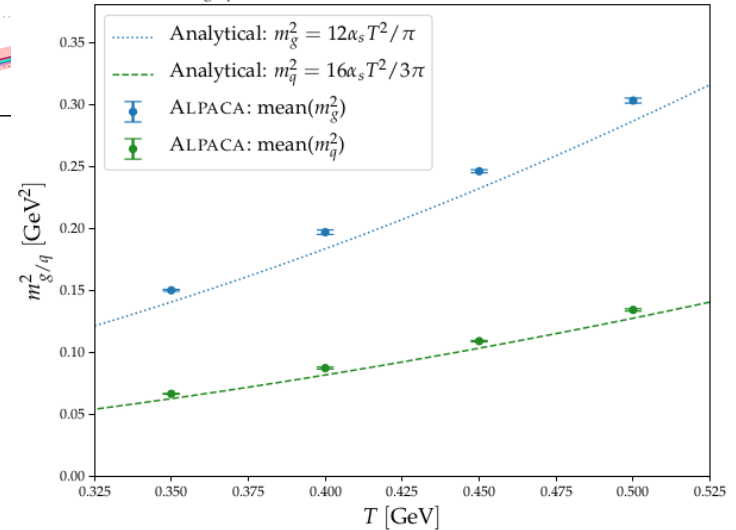
Quark Screening Mass



Gluon Screening Mass



$m_{g/q}^2$ vs T , purely gluonic system, $N_{inc} = 25$



- EKT also suffers from the same deviation at high T region.
- Note that plot on the right also used $\alpha_s = 0.3$ and periodic boundary box.
- The paper argues that this is due to the discretization of the particle density, however this discussion is outside the scope of this presentation.

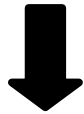
Screening Mass in 2 → 3 process

We also need to be careful with infrared divergence in 2 → 3 process.

$$\sigma_{2 \rightarrow 3} = \frac{1}{256 \pi^4} \frac{1}{\nu} \frac{1}{s} \int_0^{s/4} dq_{\perp}^2 \int_0^{s/4} dk_{\perp}^2 \int_{y_{\min}}^{y_{\max}} dy \int_0^{\pi} d\phi |\overline{\mathcal{M}}_{2 \rightarrow 3}|^2 \sum \left(\frac{\partial F}{\partial y_3} \Big|_{F=0} \right)^{-1}$$

With $|M_{2 \rightarrow 3}|^2 = 12 g^2 |M_{2 \rightarrow 2}|^2 (1-x)^2 \left[\frac{k_{\perp}^2}{k_{\perp}^2 + x^2 M^2} + \frac{q_{\perp} - k_{\perp}}{(q_{\perp} - k_{\perp})^2 + x^2 M^2} \right]$

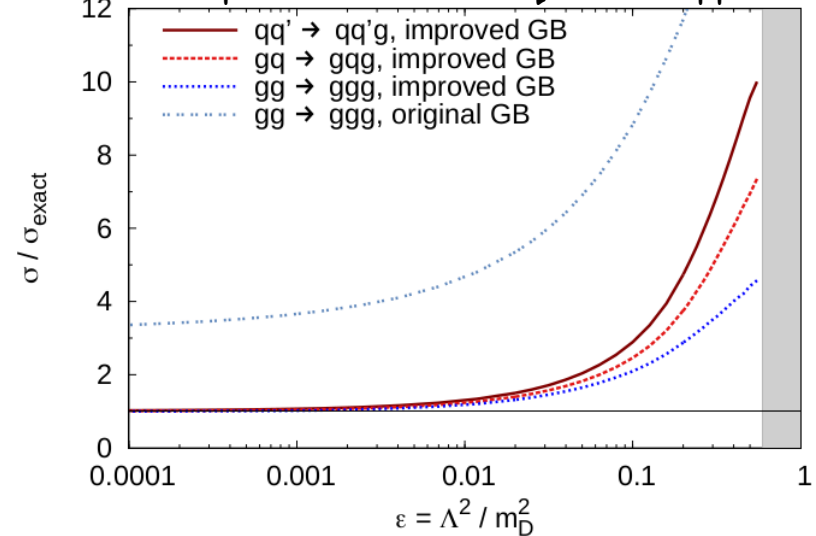
Infrared divergence



Apply cut-off as

$$\Lambda^2 = \varepsilon m_D^2 \quad \text{With } m_D \text{ is Debye Mass and } \varepsilon = 0.001$$

Comparison of Exact eq and GB approx*



Gluon absorption and radiation

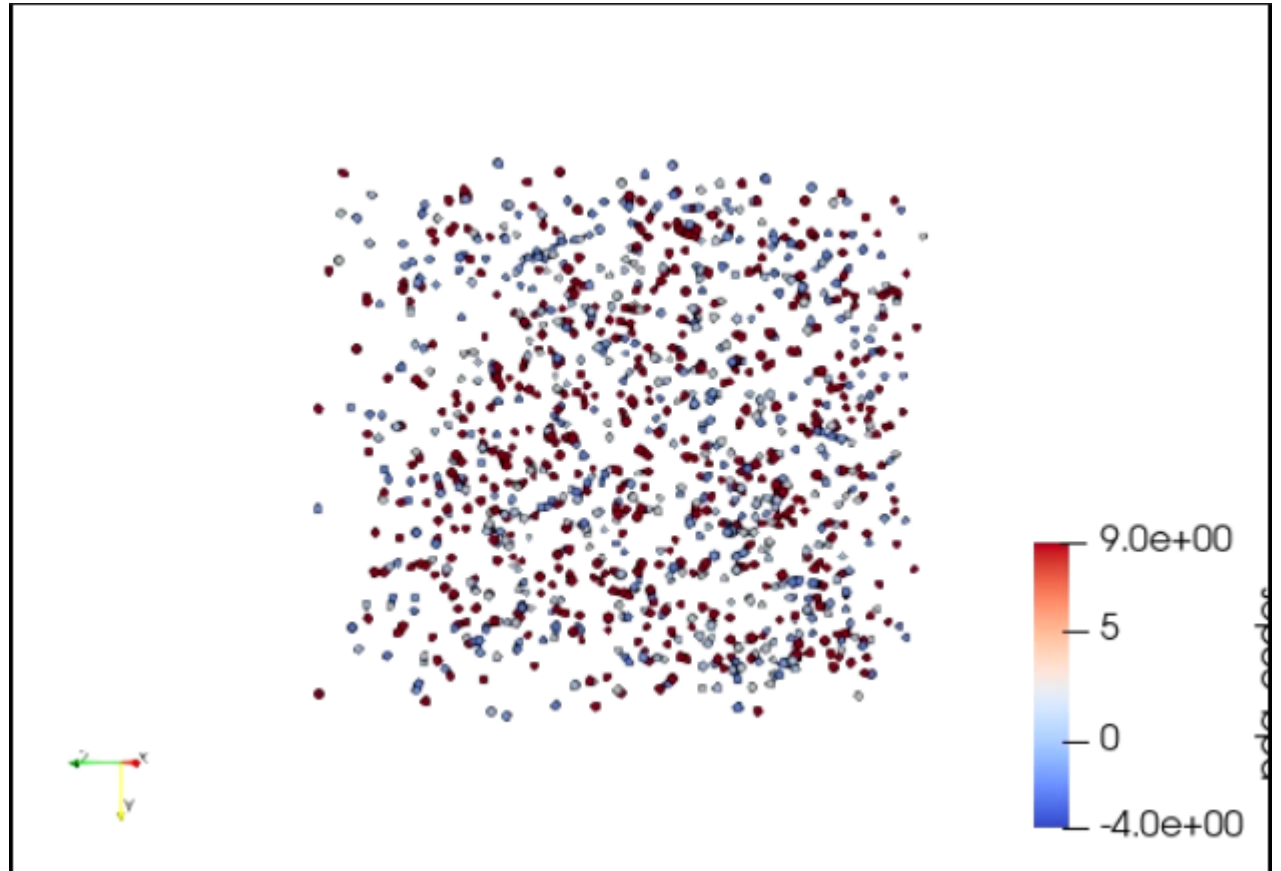
- Elastic channels preserve the total number of partons
 - Temperature describes the relation between particle number and partial energy
- => Thus there is a need to add extra channels for kinetic and chemical equilibration
- It has been shown in past calculations both from theoretical calculation^[6] and simulation^[7] that without absorption/radiation channels, medium will form condensate instead of approaching to Boltzmann distribution function.
 - In the model, we included these channels :
 - $gg \leftrightarrow gg$
 - $gq \leftrightarrow gq$
 - $qq \leftrightarrow qq$
 - $gg \leftrightarrow qq_{\text{bar}}$
 - $gg \leftrightarrow ggg$

[6] Jean-Paul Blaizot, Francois Gelis, Jinfeng Liao, Larry McLerran, Raju Venugopalan. arXiv:1107.5296 [hep-ph]

[7] Zhe Xu, Kai Zhou, Pengfei Zhuang, Carsten Greiner. arXiv:1410.5616 [hep-ph]

Simulation Setting

- Box simulation with periodic boundary condition and 3 fm box length.
- Initial condition
 - Uniform spatial distribution inside the box.
 - From mini-jet model for Au-Au @ 200 GeV and jet cut-off @ 2 GeV
- 500 gluons + 0 quark
- $E_{tot} = 1378 \pm 14$ GeV
- Note : Coupling constant is fixed at $\alpha_s = 0.3$



Result : Chemical Equilibration

- Given that energy is preserved and using Boltzmann distribution function as

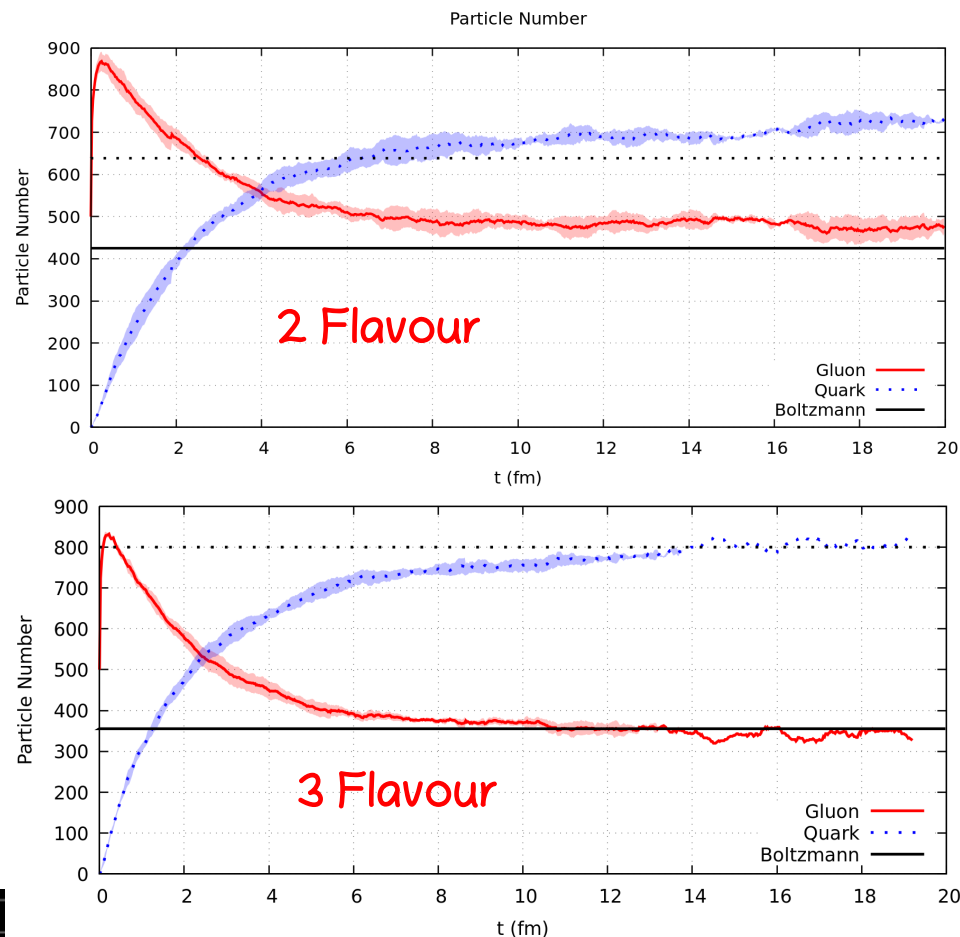
$$N_{q/g} = v_{q/g} \frac{V}{\pi^2} \left(\frac{E}{V} \frac{\pi^2}{3(v_g + v_q)} \right)^{\frac{3}{4}}$$

- 3 flavour case showed a better agreement with the Boltzmann limit.

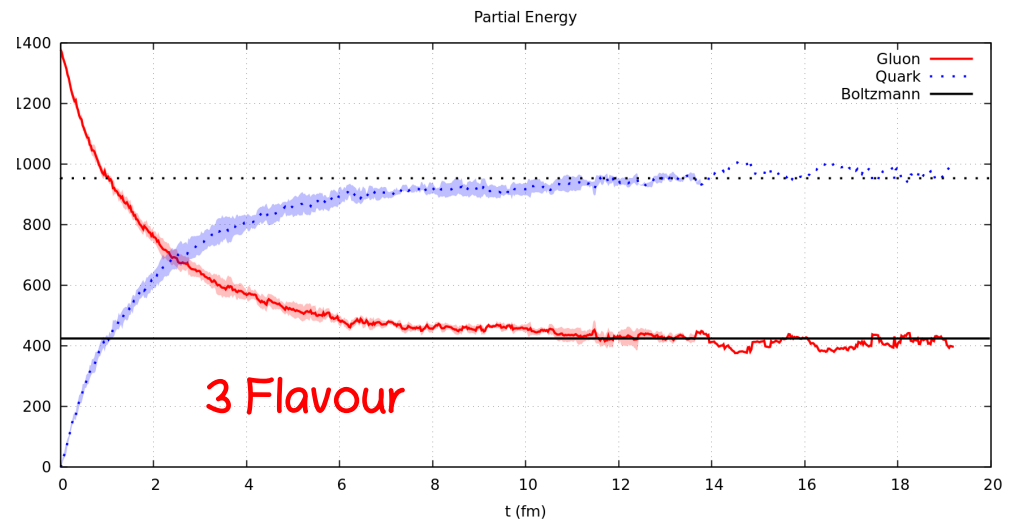
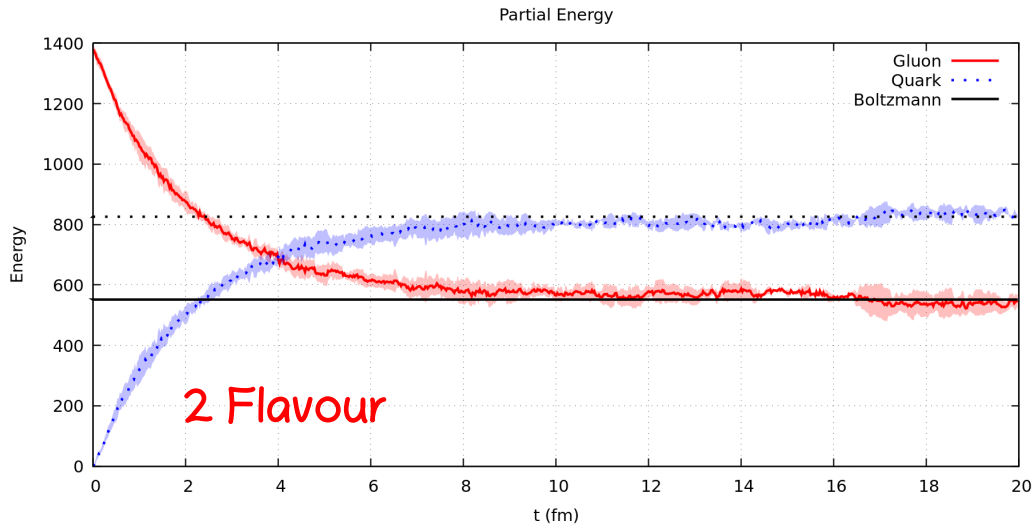
While 2 flavour case showed saturation slightly higher than Boltzmann limit.

- Chemical equilibration seems to be faster in 3 flavour case than in 2 flavour case,

This is due to the stronger $gg \rightarrow q\bar{q}$

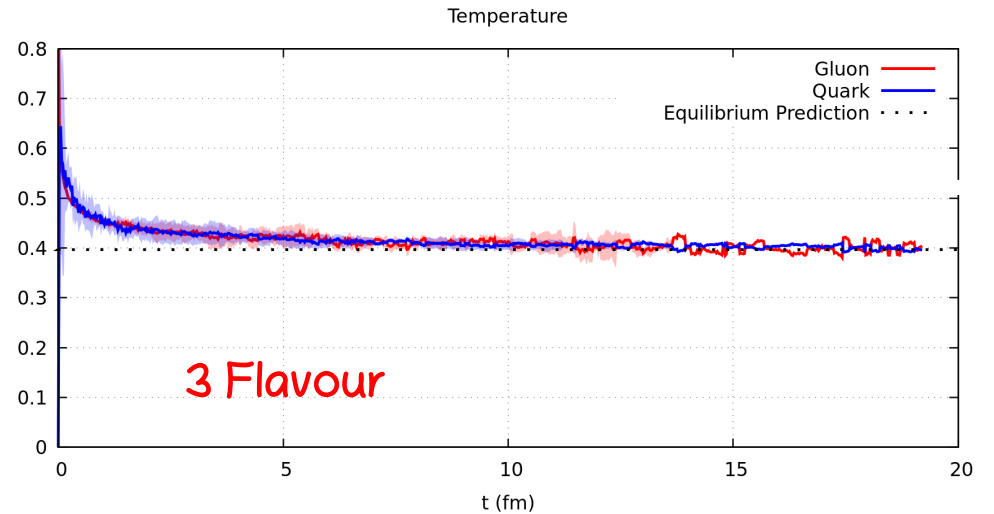
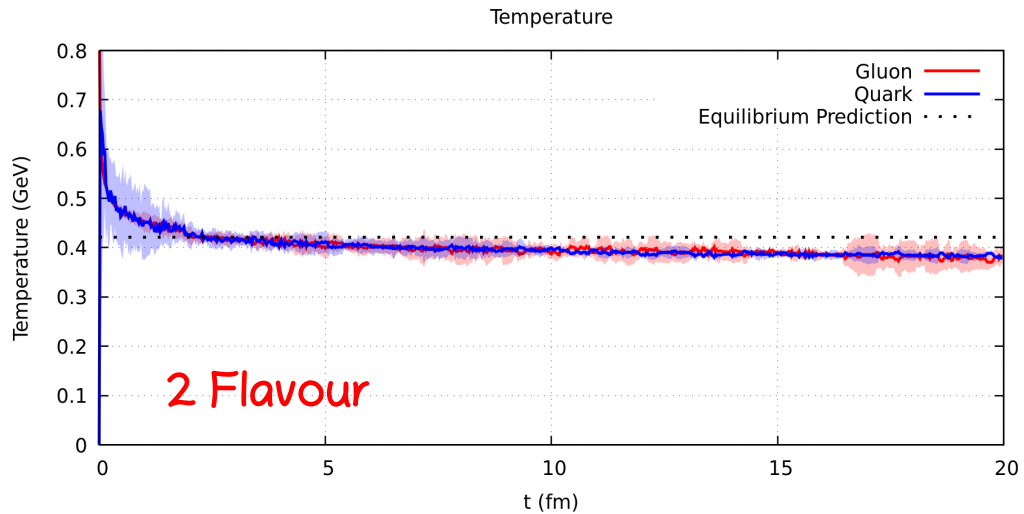


Result : Partial Energy



- In contrast to the parton number case, partial energy for both 2 flavour and 3 flavour medium saturated to the Boltzmann limit well.
- Given that partial energy and parton number saturated and are stable, it is sufficient to say that stable thermal and chemical equilibrium are achieved.

Result : Thermalization

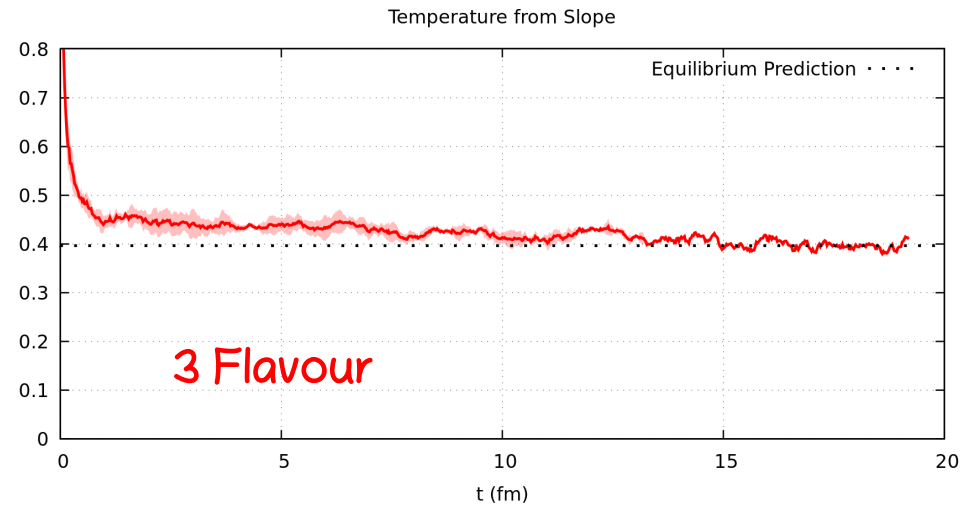
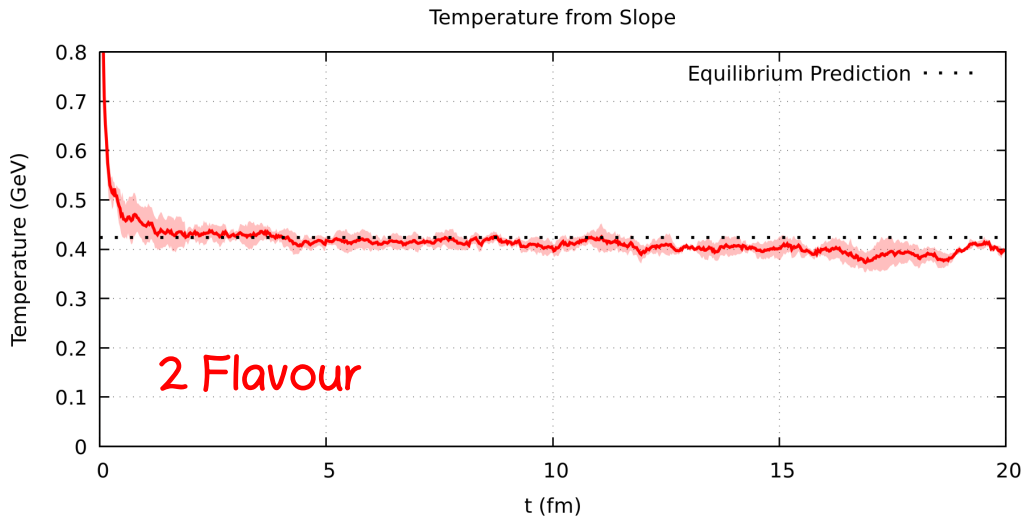


- Since thermalization is decided based on medium temperature and there is no clear definition of temperature as yet, in this case, we consider two different methods to define temperature.
- Assuming that equilibrium distribution function follows Boltzmann distribution function, temperature can be defined as the ratio of energy and parton number

$$T = \frac{1}{3} \frac{E}{N}$$

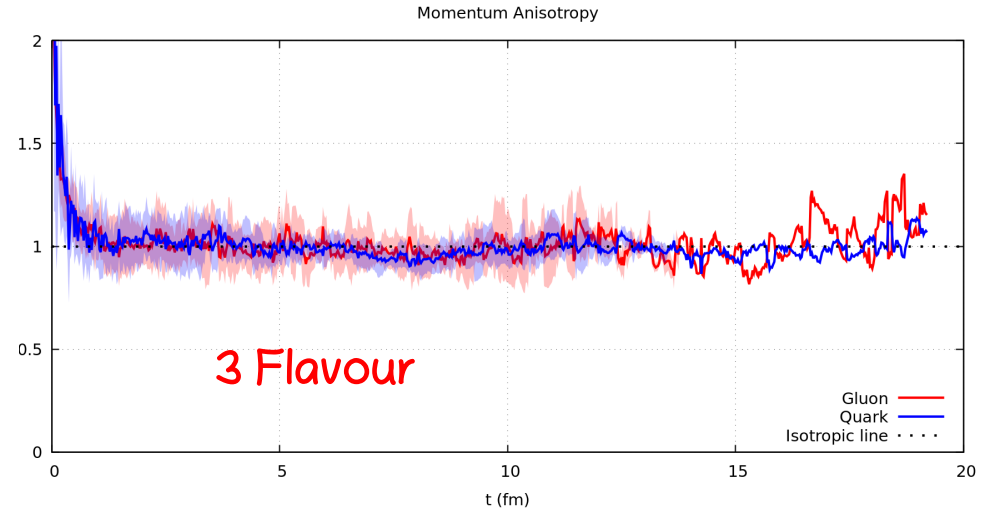
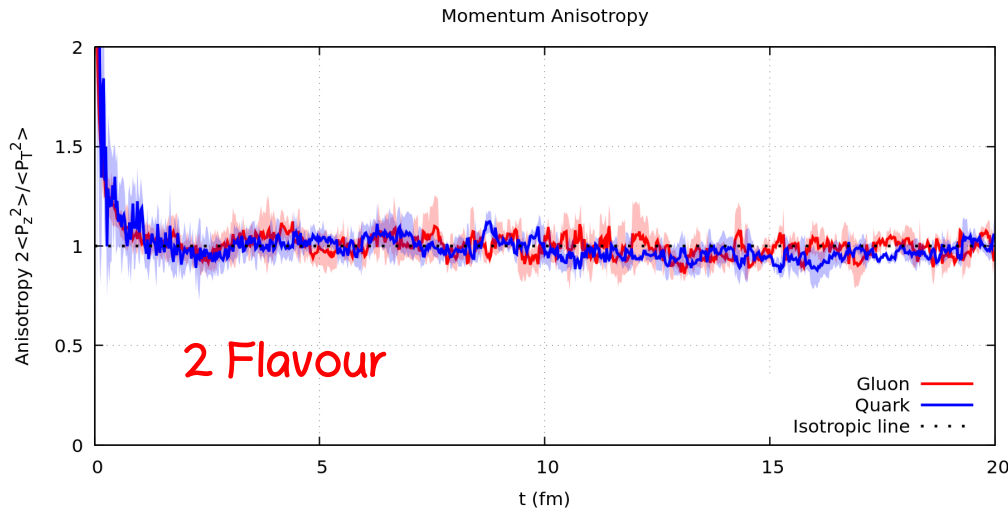
Result : Thermalization

- Temperature can also be calculated from the energy spectrum, and similarly, by assuming equilibrium state follows Boltzmann distribution, we can define temperature as the slope in logarithmic plot of energy spectrum.



- Both 2 flavour and 3 flavour cases show saturation close to predicted temperature assuming Boltzmann distribution function, and similarly as the previous method, 2 flavour saturated slightly lower than the predicted temperature while 3 flavour saturated well to the predicted value.

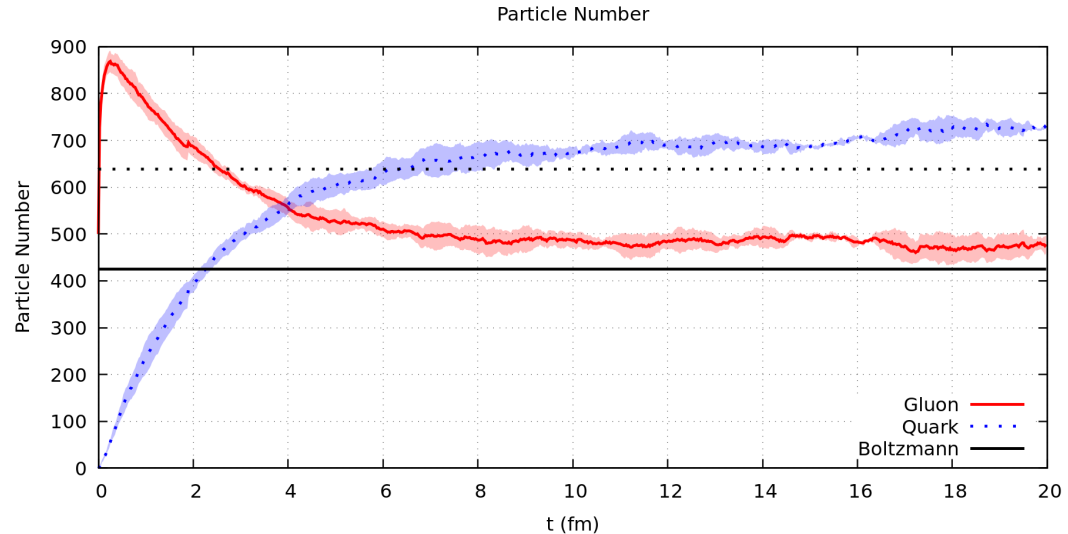
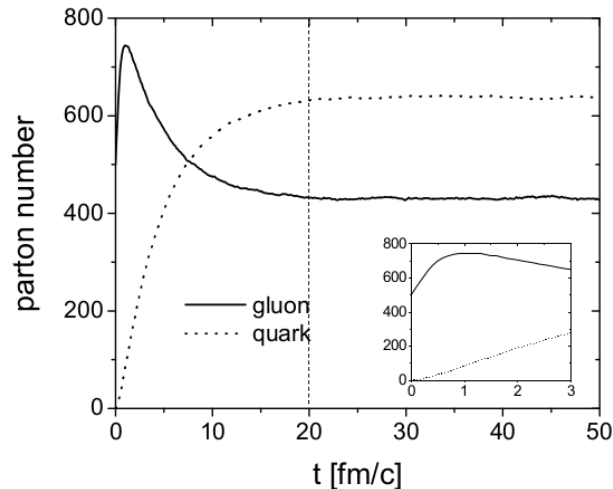
Result : Momentum Isotropization



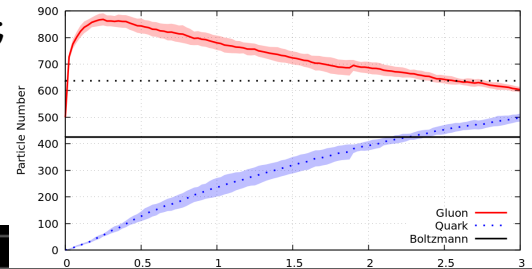
- Momentum isotropy is often considered as one of the indicators in hydrodynamization and kinetic equilibration.
- Both 2 flavour and 3 flavour medium isotropized very early. However this does not mean the medium hydrodynamized at the same time scale since the shift to hydrodynamic point of view requires the medium to reach a stable equilibrium state.

Comparison with BAMPS : Chemical Equilibration

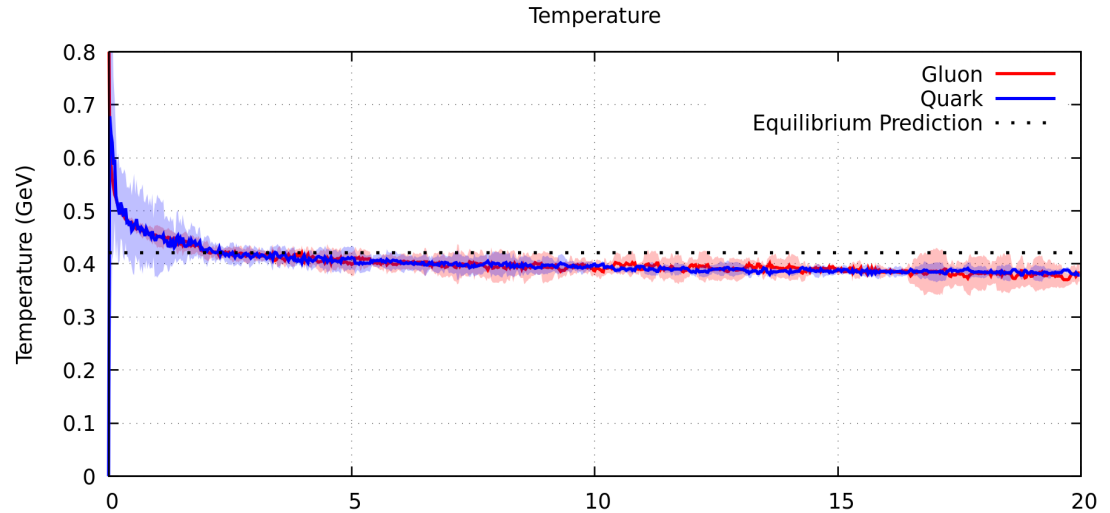
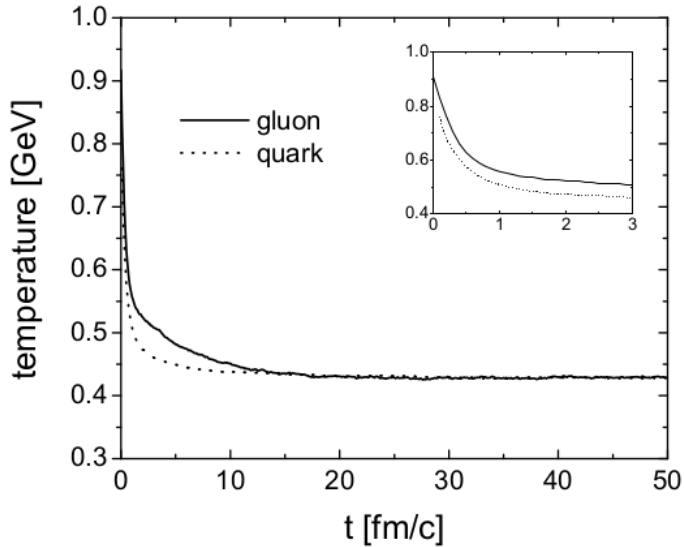
BAMPS^[8] is a well-established parton cascade model, thus comparison with BAMPS should be able to serve as a good benchmark for our parton cascade model.



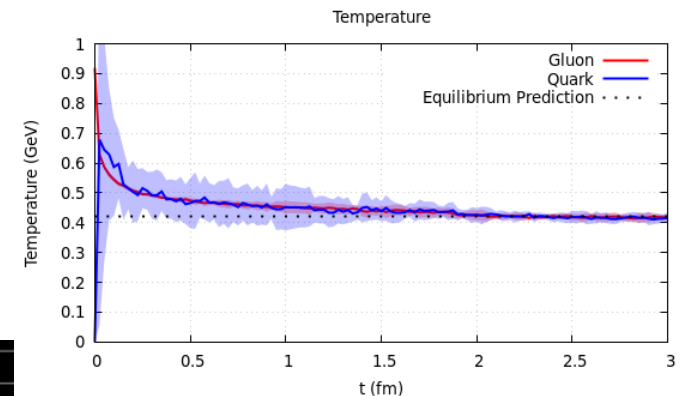
- Parton number saturates around the same time-scale for both model albeit in our model, parton number saturates slightly higher than Boltzmann limit.
- However, gluon production and quark-antiquark pair production in our model is obviously stronger than in BAMPS.



Comparison with BAMPS : Thermalization



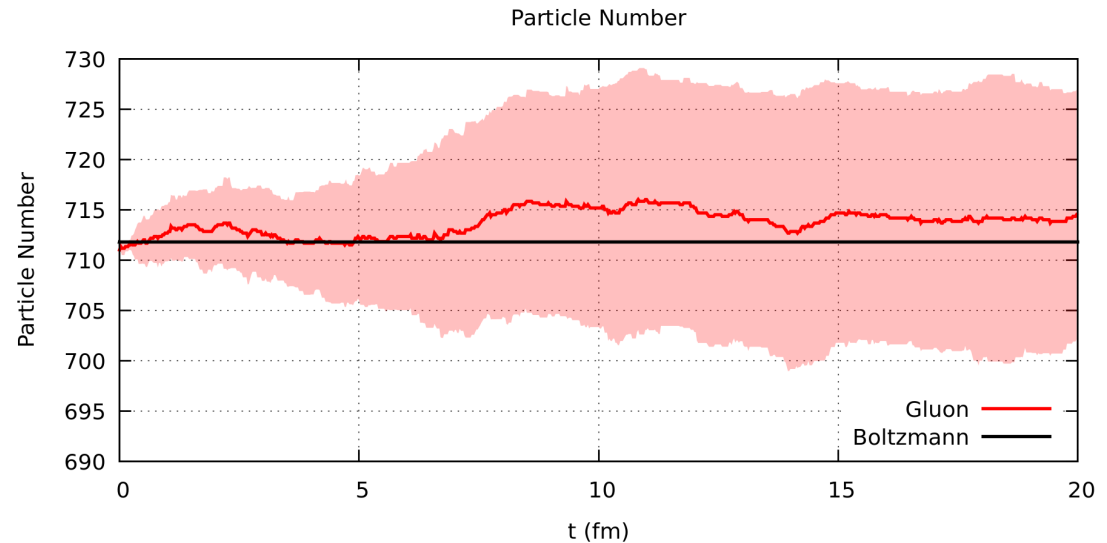
- BAMPS shows slower thermalization and different thermalization rate between gluon and quark with gluon thermalizes slower than quark.



On-going work: Extension to $qg \leftrightarrow qgg$ and $qq \leftrightarrow qqg$ processes

- The main problem with parton cascade model is the long equilibration time. As the main driving force of equilibration is inter-particle interaction, thus adding more interactions should speed up this process.
- As a preliminary check, detailed balance dictates parton number should be stable at an equilibrium state.
- Initializing a $(3 \text{ fm})^3$ box in an equilibrium state with temperature 450 MeV, and allowed interaction channels :
 - $gg \leftrightarrow ggg$
 - $qg \leftrightarrow qgg$
 - $qq \leftrightarrow qqg$

Here we see that detailed balance is satisfied
 \Rightarrow Next step would be to apply this starting from a far-from-equilibrium initial state.



Summary

- We have made a partonic transport model using stochastic collision model with 2-to-2 and 2-to-3 interactions up until leading order.
- Initial condition based on binary collision and deep inelastic scattering gives $\sigma_{PP} = 46.3622$ mb (COMPETE prediction = 51.79 mb and STAR experiment = 54.67 mb)
- Beginning from a far-from-equilibrium state, the medium's parton number and temperature saturated toward Boltzmann distribution.
- In overall, thermal and chemical equilibration are slightly faster than a well-established parton cascade model BAMPS.
- Strictly speaking, the model has two parameters
 - Mini jet momentum cut-off \Rightarrow affect initial condition parton number and total energy
 - Coupling constant $\alpha_s \Rightarrow$ affect interaction rate

Future Prospects

- Replacing the fixed coupling constant with running coupling constant

$$\alpha_s(Q^2) = \alpha_s(s) = \frac{12 \pi}{(33 - 2 n_f) \ln(s/\Lambda_{QCD}^2)}$$

However, there is a risk of inconsistency since cross sections are calculated with perturbative QCD which might not be valid when considering low s or low temperature region.

- In $2 \rightarrow 3$ calculation, we considered Feynmann diagram up to α_s^3 order, naturally, one could argue to include $2 \rightarrow 1$ process up to 1-loop correction for the sake of consistency.
- Application to heavy quark energy loss in quark gluon plasma.
Compare to theoretical predictions of heavy quark energy loss from both elastic* and radiative** processes.
- Connection to hydrodynamic model.
The main challenge here is to connect the discrete theory of kinetic theory to the continuous theory of hydrodynamic.
One common approach is to use Gaussian smearing, however this introduces Gaussian smearing width, a non-physical parameter.

*Peigne and Peshier (arXiv:0802.4364)

**R. Abir, U. Jamil, M. G. Mustafa, D. K. Srivastava, Phys. Lett. B 715, 183 (2012).

THANK YOU!